Tables 3.1. Table 3.2 presents the Fortran listing of the main program and all the subroutines. The program can be run on any Fortran complier and the dimensions of various quantities can be increased, if required, within the capability of complier and operating system. Sample data and result for a plate loaded as a cantelever are as given.

REFERENCES

1. Pipes, L.A. and Harvill, L.R. 1970. *Applied Mathematics for Engineers and Physicists*. McGraw-Hill Book Co., Kogakusha Ltd.
2. Chapra, S.C. and Canale, R.P. 1970. *Numerical Methods for Engineers, with PC Applications*. McGraw-Hill Book Co., N.Y.

Chapter 4

VARIATIONAL APPROACH AND HEAT-FLOW ANALYSIS (POTENTIAL PROBLEM)

4.1 INTRODUCTION AND APPLICATION EXAMPLES

Heat transfer by conduction, convection and radiation plays a vital role in many engineering applications. The traditional approach to solving these problems relies heavily on providing the solution for a highly simplified model, leaving the user to interpret from these results an application to a realistic complex situation. Often this approach doesn't work and predictions are far away from reality. For illustration, consider the simple example shown in Fig. 4.1. The analytical and experimental

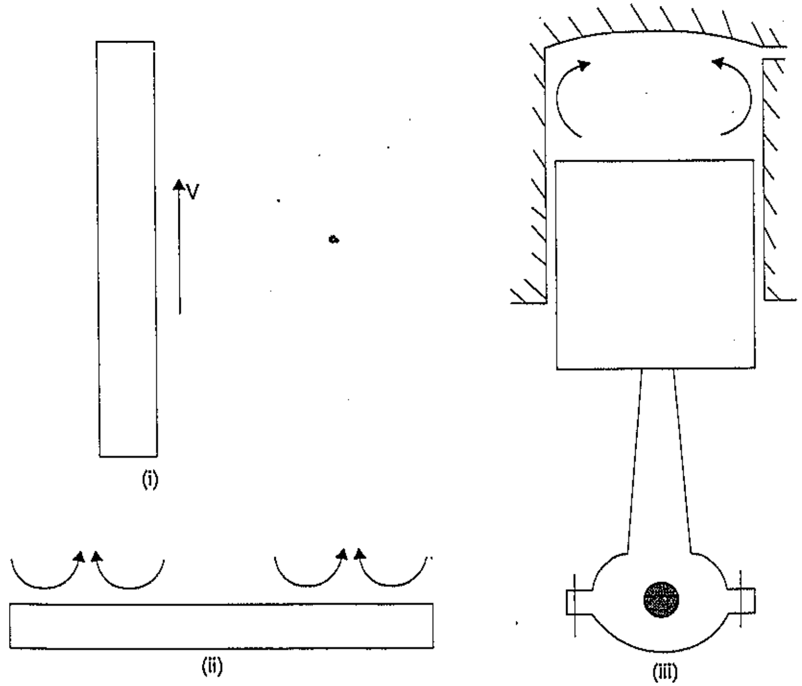

Fig. 4.1 Modes of heat convection

solutions are available for convective heat transfer from large vertical plates (i) and horizontal plates (ii). The air (or gas) velocity v is assumed constant and convective heat transfer coefficient is determined. A realistic situation is shown in (iii) where we are interested in the heating of an engine cylinder and piston due to heat transfer from gases produced by combustion. All the parameters, such as gas velocity and temperature, surface temperature on cylinder walls and piston are not known and vary widely. The results available for the heat transfer coefficient from vertical and horizontal plates provide no clue to the real heat transfer coefficient on the walls of the cylinder-piston assembly. Use of any such factor will make the results highly unrealistic. This example illustrates the limitations of the traditional approach.

The finite element method takes care of the situation as it exists in reality. A proper finite element analysis strategy will involve first determination of the gas flow pattern and convective heat transfer in the combustion chamber. The solution should then be obtained for heat transfer by conduction in the cylinder and piston. Later, mutual interaction of the convective and conductive heat transfer at every point in the region should be analyzed. Several iterations are required to obtain the correct result. There are many more situations to which the finite element modelling of heat transfer phenomena is applied successfully. Figure 4.2 illustrates a few of them. Cooling through fins of varying thickness and size in the engine cylinder block, compressor etc., modelling of temperature distribution in various zones of baking ovens used for curing paint or furnaces used for heating parts for heat treatment and heating the components during induction hardening (Fig. 4.2(a), (b), (c)) are some of the application examples in production. There are many situations in the field of material processing wherein thermal finite element modelling has been used very successfully. Examples are:

(a) Cooling of billet during continuous casting in steel plants[1] in which molten metal comes out of the mould in the form of a long continuous solidifying strand which may be used directly for the purpose of rolling, thus avoiding expensive reheating of the billet before rolling. However, if the thermal conditions are not proper the solidifying skin of the billet may rupture under the pressure of molten metal within and thus strict control of the cooling operation is required.

(b) The metal flow during forging is highly dependent on the temperature prevailing in various regions of the forged component. Final mechanical properties of the forged component and crack formation also depend greatly on the temperature distribution in it. (Fig. 4.2(d)). Pillinger et al.[2] have reported an approach for finite element modelling of the forging operation.

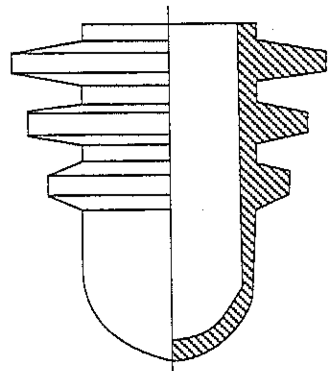

(a) Cooling fins

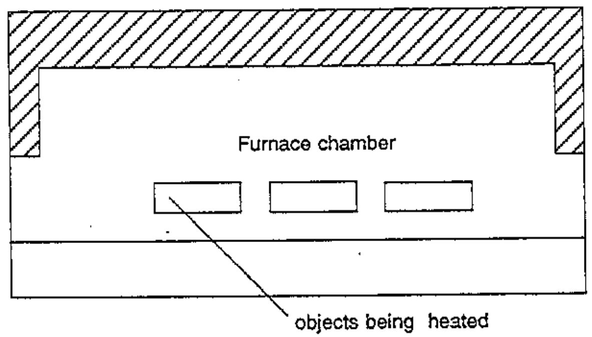

(b) Oven for drying paint or furnace for heat treatment

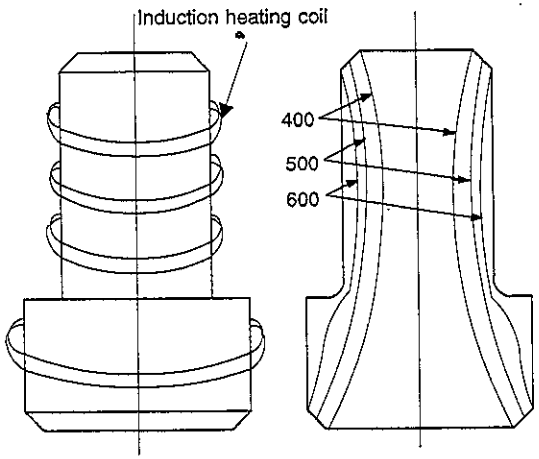

(c) Induction hardening of a stepped shaft Isotherms over the cross-section

Fig. 4.2

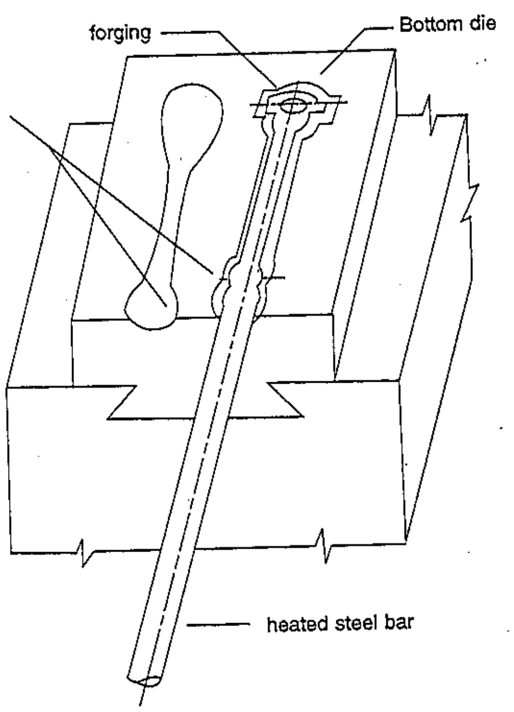

(d) Forging

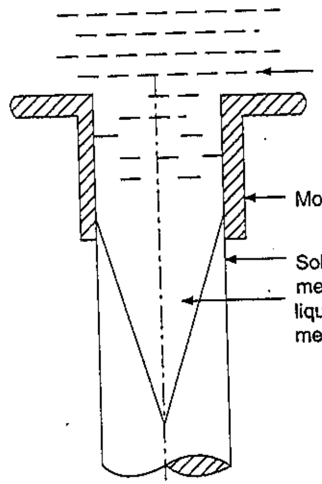

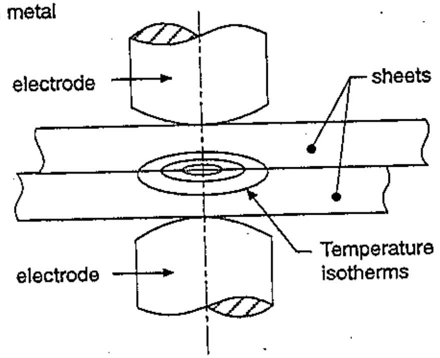

(f) Resistance welding

(e) Continuous casting of steel billet in steel making

Fig. 4.2 Applications of thermal F.E. analysis.

(c) The growth of a fused weld spot in resistance spot welding has also been analyzed using FEM through thermal modelling[3].

These are only a few examples from the wide spectrum of applications to which thermal FE modelling is applied.

4.1.1 General Procedure

The governing equation of heat conduction in moving fluids is given as,

$$\frac{\partial T}{\partial \tau} + u\frac{\partial T}{\partial x} + v\frac{\partial T}{\partial y} + w\frac{\partial T}{\partial z} = \frac{k}{c\rho}\left(\frac{\partial^2 T}{\partial x^2} + \frac{\partial^2 T}{\partial y^2} + \frac{\partial^2 T}{\partial z^2}\right) + \frac{\dot{Q}}{c\rho}^{(1)} \quad \dots (4.1)$$

Here u, v and w are fluid velocities in Cartesian coordinate directions x, y and z respectively. Thermal conductivity (k), specific heat (c) and density (ρ) are material properties assumed constant in this expression. In a steady-state situation the time derivative of temperature ($\partial T/\partial \tau$) will be zero. Thus for a stationary medium ($u = v = w = 0$) the steady-state heat conduction equation reduces to,

$$k\left(\frac{\partial^2 T}{\partial x^2} + \frac{\partial^2 T}{\partial y^2} + \frac{\partial^2 T}{\partial z^2}\right) + \dot{Q} = 0 \quad \dots (4.2)$$

In this expression $\dot{Q}$ represents the rate of heat generation in unit volume. Besides satisfying the governing equation (4.1 or 4.2) the heat flow should also satisfy boundary conditions, which may be specified as constant temperature at the boundary or as known temperature gradient normal to the boundary, specifying surface heat transfer in a unique manner. Expressed mathematically these are

$$T = T_0 \text{ at } S_1$$

$$\frac{\partial T}{\partial n} = f(T) \text{ at } S_2 \text{ or, } k\frac{\partial T}{\partial n} + \alpha T + q = 0 \quad \dots (4.3)$$

where S_1 and S_2 represent the portions of the boundary on which these two boundary conditions are specified. For unsteady-state heat flow an

---

[1] For temperature dependent thermal properties or when therml conductivity shows directional behaviour and its magnitudes are k_x, k_y and k_z in the three directions, we use the more general relationship given as,

$$c\rho\left[\frac{\partial T}{\partial \tau} + u\frac{\partial T}{\partial x} + v\frac{\partial T}{\partial y} + w\frac{\partial T}{\partial z}\right] =$$

$$\frac{\partial}{\partial x}\left(k_x\frac{\partial T}{\partial x}\right) + \frac{\partial}{\partial y}\left(k_y\frac{\partial T}{\partial y}\right) + \frac{\partial}{\partial z}\left(k_z\frac{\partial T}{\partial z}\right) + \dot{Q}$$

additional condition specifies the temperature at the beginning ($\tau = 0$). This is known as the initial condition, expressed in the form,

$$T = T_{i0} \quad \text{at } \tau = 0 \qquad \text{... (4.4)}$$

We shall begin with the steady-state heat conduction equation in stationary objects (eq. 4.2) under the boundary conditions given by eqs. (4.3). Equations governing several other phenomena, such as electromagnetic field distribution, current density distribution or flow of inviscid fluids are similar in form. Thus equations of the form given by (4.2) govern a large class of problems known as potential problems and the formulation for all of them follows a similar procedure.

If we compare the present problem with the stress analysis in solid bodies discussed in Chapter 2, we immediately observe that the presence of potential energy as an optimizing function helped in the formulation there. Since the equilibrium state was known to be the one for which total potential energy of the system was minimum, it was found convenient to express total potential energy in an integral form. Minimization of this potential energy resulted in a set of simultaneous equations which yielded the final solution. In the present case we unfortunately do not have a known physical quantity which gives the solution on minimization. However, variational calculus provides us with a means of establishing a mathematical function, which on minimization gives the solution of a governing equation such as (4.2). The next section deals with some aspects of variational calculus which are relevant to the formulation of this problem.

4.2 FUNDAMENTALS OF VARIATIONAL CALCULUS

Since we are already aware of the method used for analyzing stresses in a body for which potential energy is minimized in order to obtain a solution, we may look at this expression to take guidance regarding the nature of the function normally encountered. Strain energy contains terms like $\partial\overline{u}/\partial x$, $\partial\overline{v}/\partial y$ etc. and we may logically assume that the function to be minimized will contain some parameters (here displacement $\overline{u}, \overline{v}$) and their derivatives ($\partial\overline{u}/\partial x$, $\partial\overline{v}/\partial y$ etc.) in addition to being a function of coordinates. Thus, in general the function can be expressed as the following domain integral,

$$I = \int_V F\left(x, y, z, \overline{u}, \overline{v}, \overline{w}, \frac{\partial\overline{u}}{\partial x}, \frac{\partial\overline{u}}{\partial y}, \ldots \frac{\partial\overline{v}}{\partial x}, \ldots \frac{\partial\overline{w}}{\partial x}, \ldots\right) dV \qquad \text{... (4.5)}$$

We may logically conclude that the function to be minimized for the case of thermal analysis should contain temperature (T) and its gradients. It can be expressed as

$$I = \int_V F\left(x, y, z, T, \frac{\partial T}{\partial x}, \frac{\partial T}{\partial y}, \frac{\partial T}{\partial z}\right) dV$$

$$= \int_V F\left(x, y, z, T, T_x, T_y, T_z\right) dV \qquad \text{... (4.6)}$$

Here partial differentials are symbolically represented by T_x, ... etc. Again, specializing the case to a one-dimensional problem (say, temperature distribution in a rod) the above expression is rewritten as

$$I = \int_{x_1}^{x_2} F(x, T, T_x)\, dx, \qquad \text{... (4.7)}$$

where x_1 and x_2 are the values of x at the two ends of the rod. It now becomes possible to pose the problem under investigation in mathematical form. For simplicity we consider a one-dimensional problem. Equation (4.7) provides us with a clue. Interpreted logically, it can be stated that like potential energy we should find a function $F(x, T, T_x)$ whose integral over the length of rod as given by eq. (4.7), when minimized, gives the solution. Here the solution obviously implies that the governing equation of heat conduction is satisfied at all the points in the rod and the boundary conditions are satisfied at the ends of the rod.

We shall now try to perform minimization of integral I given by eq. (4.7). A look at function $F(x, T, T_x)$ reveals that it is not a simple function of coordinates which can be minimized by equating to zero the partial derivatives with respect to the coordinates. Here both T and T_x ($\partial T/\partial x$) are themselves the functions of coordinates (x in one-dimensional case). Hence F is a function of functions. In mathematical terminology it is called a functional to differentiate it from simple function.

4.2.1 Minimization of Functional

As stated above, a functional is not a simple function and its minimization will not follow the usual procedure. We proceed in the following manner for its minimization. Figure 4.3 shows the distribution of T and $F(x, T, T_x)$ in the range $x_1 - x_2$. If the distributions shown by solid lines are the solutions to the problems which we have to obtain, we consider an adjoining distribution of T (i.e., $\overline{T}$) which is very close to T and which is obtained by adding the product of a small number ε and another function of x (given as n), which is also defined in the range $x_1 - x_2$. Or

$$\overline{T} = T + \varepsilon n \text{ (at all points in range } x_1 \rightarrow x_2)$$

This functional $\overline{T}$ gives another distribution of F as $\overline{F}$. The differential of $\overline{T}$ with respect to x can be written as

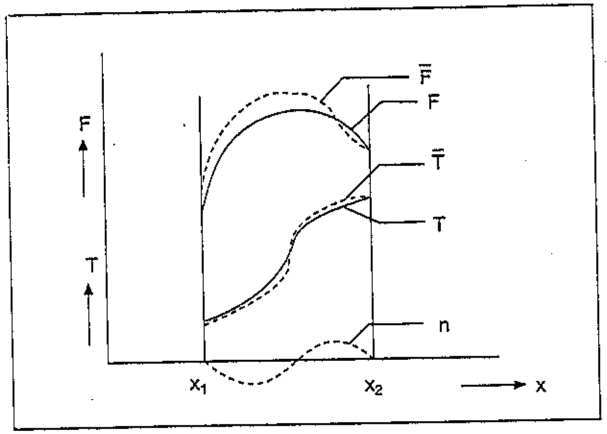

Fig. 4.3

$$\overline{T}_x = T_x + \varepsilon n_x \left(\text{or, } \frac{dT}{dx} + \varepsilon \frac{dn}{dx} \right) \quad \text{... (4.8)}$$

Functional $\overline{F}$, which is a nearby function to F, can be written as,

$$\overline{F}\,(x, T + \varepsilon n, T_x + \varepsilon n_x) \quad \text{... (4.9)}$$

or (alternatively),

$$\overline{F}\,(x, \overline{T}, \overline{T}_x) \quad \text{... (4.5a)}$$

We may observe that $\overline{T}$ is an arbitrary distribution of temperature and can take various values just by changing ε, even though both T and n remain fixed and specified functions of x. $\overline{F}$ may thus be treated as a function of only one variable ε and even then the minimization of $\overline{F}$ should give a distribution of T which is the solution to the given problem. Minimization of $\overline{F}$ which is now a simple function of variable ε is obtained by using the condition,

$$\frac{dI}{d\varepsilon} = 0 \quad \text{... (4.10)}$$

or,

$$\int_{\substack{x_1 \\ \varepsilon \to 0}}^{x_2} \frac{d}{d\varepsilon} \{\overline{F}\,(x, \overline{T}, \overline{T}_x)\}\, dx = 0$$

or,

$$\int_{\substack{x_1 \\ \varepsilon \to 0}}^{x_2} \left[\frac{\partial \overline{F}}{\partial \overline{T}} \frac{\partial \overline{T}}{\partial \varepsilon} + \frac{\partial \overline{F}}{\partial \overline{T}_x} \frac{\partial \overline{T}_x}{\partial \varepsilon} \right] dx = 0. \quad \text{... (4.11)}$$

Since by assumption $\overline{F}$ is the same function of $\overline{T}$ and $\overline{T}_x$ as F is of T and T_x, we can write

$$\underset{\text{as } \varepsilon \to 0}{\frac{\partial \overline{F}}{\partial \overline{T}} = \frac{\partial F}{\partial T}} \quad \text{and} \quad \underset{\text{as } \varepsilon \to 0}{\frac{\partial \overline{F}}{\partial \overline{T}_x} = \frac{\partial F}{\partial T_x}} \quad \text{... (4.11)}$$

We also have

$$\frac{\partial \overline{T}}{\partial \varepsilon} = \frac{\partial\,(T + \varepsilon n)}{\partial \varepsilon} = n$$

and,

$$\frac{\partial \overline{T}_x}{\partial \varepsilon} = \frac{\partial\,(T_x + \varepsilon n_x)}{\partial \varepsilon} = n_x$$

On substituting in eq. (4.11) we obtain,

$$\int_{x_1}^{x_2} \left[\frac{\partial F}{\partial T} n + \frac{\partial F}{\partial T_x} n_x \right] dx = 0 \quad \text{... (4.12)}$$

Integrating the second term by parts

$$\int_{x_1}^{x_2} \frac{\partial F}{\partial T_x} \frac{dn}{dx} dx = \left[n \frac{\partial F}{\partial T_x} \right]_{x_1}^{x_2} - \int_{x_1}^{x_2} n \frac{d}{dx} \left(\frac{\partial F}{\partial T_x} \right) dx$$

The first term on the right side becomes zero because the value of n is zero at both the ends, $x = x_1$ and $x = x_2$, due to the assumed nature of function n. On substituting the second term in eq (4.12) we obtain

$$\frac{dI}{d\varepsilon} = \int_{x_1}^{x_2} \left[\frac{\partial F}{\partial T} - \frac{d}{dx} \left(\frac{\partial F}{\partial T_x} \right) \right] n \cdot dx = 0 \quad \text{... (4.13)}$$

Since n is an arbitrary function of x which can have any independent value at any points between x_1 and x_2 the only way in which the integral stated in equation (4.13) can be zero is that the term within brackets be zero at all the points in the range x_1 to x_2 or,

$$\frac{\partial F}{\partial T} - \frac{d}{dx} \left(\frac{\partial F}{\partial T_x} \right) = 0 \text{ (at all points in the domain)} \quad \text{... (4.14)}$$

The implication of this derivation is that minimization of the integral of functional F within the specified domain (here range $x_1 \forall x_2$) is equivalent to satisfying eq. (4.14) at all the points of domain.

4.2.2 Euler-Lagrange Equation

We have derived above the essential condition for the integral of a functional F to attain a minimum. For a one-dimensional problem involving one variable T it is stated in the form of eq. (4.14). This is called the *Euler-Lagrange (or Euler) equation.*

We can easily extend it to two- or three-dimensional cases involving more than one variable (such as $\bar{u}, \bar{v}, \bar{w}$). The functional will then be stated in the form of expressions (4.5) or (4.6). We shall now derive the Euler equation for a two-dimensional case involving only one variable T. Before taking up this derivation it is useful to consider the implication of the Euler equation in the context of finite element analysis. The governing equation of one-dimensional steady state heat conduction is given as,

$$k\frac{d^2T}{dx^2} + \dot{Q} = 0 \qquad \text{... (4.15)}$$

Here k is thermal conductivity and $\dot{Q}$ is the rate of internal heat generation. This equation should be satisfied at all the points of the one-dimensional rod under consideration. Since an essential condition for minimization of integral of a functional F is that the Euler equation (eq. 4.14) be satisfied at all the points of domain, we may say that for a one-dimensional heat conduction problem if the function F is chosen in a manner that the Euler equation becomes identical with the governing equation (eq. 4.15), then we have obtained the functional which on minimization gives the solution. It is easy to see that such functional is given by,

$$F = \frac{1}{2}k\left(\frac{dT}{dx}\right)^2 - \dot{Q}T \qquad \text{... (4.16)}$$

Coming back to the problem of establishing the Euler equation for a two-dimensional case, the domain here will be the area A shown in Fig. 4.4 which has a boundary L. In the one-dimensional problem analyzed above, a functional F was obtained which satisfied the governing equation in the domain. For a two-dimensional case we may also have the boundary condition in the form of another equation specified along boundary L in addition to the one specified in domain A. The Euler equation should now be developed with two functionals, F_1 and F_2, such that one is specified in domain A and the other on boundary L. Minimization of the sum of the integrals of two functionals along respective domains should now be established and this should yield two Euler equations, one along the domain and the other at the boundary. Thus,

$$I = \int_A F_1(x, y, T, T_x, T_y)\, dA + \int_L F_2(x, y, T, T_x, T_y)\, dL \qquad \text{... (4.17)}$$

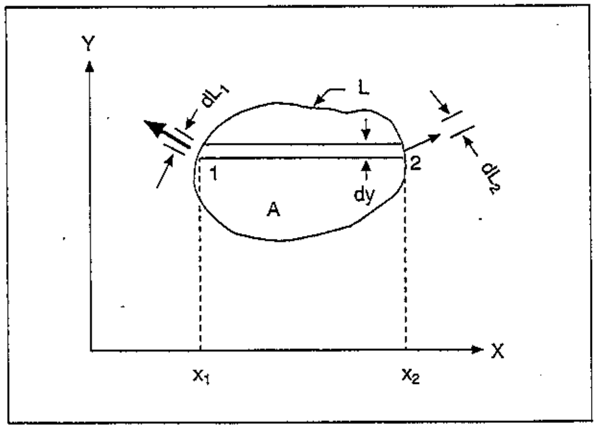

Fig. 4.4

We may again define an arbitrary function of coordinates n (i.e., $n(x, y)$) both in the domain A and on the boundary L. By using an arbitrary small quantity ε we define $\bar{T}, \bar{T}_x$ and $\bar{T}_y$ as follows along the domain as well as boundary (note that n is not zero at the boundary now).

$$\bar{T} = T + \varepsilon n;\ \bar{T}_x = T_x + \varepsilon n_x;\ \bar{T}_y = T_y + \varepsilon n_y$$

If the integral of these neighbouring functionals $\bar{F}_1$ and $\bar{F}_2$ by using $\bar{T}, \bar{T}_x$ and $\bar{T}_y$ in place of T, T_x, T_y is defined as $\bar{I}$, then minimization will be carried out by equating $d\bar{I}/d\varepsilon$ to zero. For the present if F_2 is taken as function of x, y and T only[2] then,

$$\bar{I} = \iint_A \bar{F}_1(x, y, T + \varepsilon n, T_x + \varepsilon n_x, T_y + \varepsilon n_y)\, dx\, dy + \int_L \bar{F}_2(x, y, T + \varepsilon n)\, dL \qquad \text{... (4.18)}$$

and,

$$\frac{d\bar{I}}{d\varepsilon} = \iint_A \left(\frac{\partial F_1}{\partial T} n + \frac{\partial F_1}{\partial T_x} n_x + \frac{\partial F_1}{\partial T_y} n_y\right) dx\, dy + \int_L \frac{\partial F_2}{\partial T} n\, dL = 0 \qquad \text{... (4.19)}$$

[2] The function F_2 is taken as function of coordinates and T only because the presence of terms such as T_x, T_y result in complicated expressions and the boundary conditions commonly encountered can be obtained easily by considering F_2 as function of T alone.

Considering the integral of $(\partial F_1/\partial T_x) \cdot n_x$ and simplifying it, we get

$$\int_y \int_x \frac{\partial F_1}{\partial T_x} \frac{\partial n}{\partial x}\, dx\, dy = \int_y \left[n \frac{\partial F_1}{\partial T_x} \Big|_{x_1}^{x_2} - \int_x n \frac{\partial}{\partial x}\left(\frac{\partial F_1}{\partial T_x}\right) dx \right] dy \quad \text{... (4.20)}$$

The function has been integrated by parts over a small strip of width dy extending from point 1 to 2 of domain A, as shown in Fig. 4.4. If the lengths of boundary segments at points 1 and 2 are dL_1 and dL_2 respectively, the following relationship holds good between strip width dy and dL_1 and dL_2:

$$dy = -\, dL_1 \cdot l_{x1} = dL_2 \cdot l_{x2} \quad \text{... (4.21)}$$

where l_{x1} and l_{x2} are the direction cosines of the outward drawn normals to the boundary at points 1 and 2. Substituting in (4.20), we get the first term within the integral sign on the right side as,

$$\left[n \frac{\partial F_1}{\partial T_x} l_{x2} \cdot dL_2 + n \frac{\partial F_1}{\partial T_x} l_{x1} \cdot dL_1 \right] \quad \text{... (4.22)}$$

This represents the quantity $n(\partial F_1/\partial T_x) \cdot l_x \cdot dL$ for the portion of the boundary intercepted by the strip of width dy in Fig. 4.4.

When this integral is extended over the whole range of dy as envisaged in expression (4.20), the first term of eq. (4.20) now becomes the integral of the quantity expressed above over the whole boundary. Thus

$$\int_y \left[n \frac{\partial F_1}{\partial T_x} \Big|_{x_1}^{x_2} \right] dy = \int_L n \frac{\partial F_1}{\partial T_x} l_x \, dL \quad \text{... (4.23)}$$

and expression (4.20) can be rewritten as

$$\int_y \int_x \frac{\partial F_1}{\partial T_x} \frac{\partial n}{\partial x}\, dx\, dy = \int_L n \frac{\partial F_1}{\partial T_x} l_x\, dL - \int_y \int_x n \frac{\partial}{\partial x}\left(\frac{\partial F_1}{\partial T_x}\right) dx\, dy \quad \text{... (4.24)}$$

A similar expression is obtained for integral $(\partial F_1/\partial T_y)\, n_y$ of eq. (4.19) and on substitution, eq. (4.19) becomes

$$\int_y \int_x \left[\frac{\partial F_1}{\partial T} - \frac{\partial}{\partial x}\left(\frac{\partial F_1}{\partial T_x}\right) - \frac{\partial}{\partial y}\left(\frac{\partial F_1}{\partial T_y}\right) \right] n\, dx\, dy$$

$$+ \int_L \left[\frac{\partial F_1}{\partial T_x} l_x + \frac{\partial F_1}{\partial T_y} l_y + \frac{\partial F_2}{\partial T} \right] n \cdot dL = 0 \quad \text{... (4.25)}$$

Expression 4.25 is the condition for minimization of the sum of integrals of functional F_1 and F_2 defined over the domain A and boundary L

respectively. Since n is a totally arbitrary function of coordinates x and y, the only way in which expression (4.25) can be satisfied is that the expression given in the first brackets be satisfied at all the points of domain A and the one given in the second brackets be satisfied at all the points of the boundary L. Thus again the Euler-Lagrange equation for a two-dimensional case is obtained as

$$\frac{\partial F_1}{\partial T} - \frac{\partial}{\partial x}\left(\frac{\partial F_1}{\partial T_x}\right) - \frac{\partial}{\partial y}\left(\frac{\partial F_1}{\partial T_y}\right) = 0 \text{ at all points in domain } A \quad \text{... (4.26)}$$

and $$\frac{\partial F_1}{\partial T_x} l_x + \frac{\partial F_1}{\partial T_y} l_y + \frac{\partial F_2}{\partial T} = 0 \text{ at all points on boundary } L$$

It is easy to see that extension of this analysis to a three-dimensional case will result in following Euler-Lagrange equations,

$$\frac{\partial F_1}{\partial T} - \frac{\partial}{\partial x}\left(\frac{\partial F_1}{\partial T_x}\right) - \frac{\partial}{\partial y}\left(\frac{\partial F_1}{\partial T_y}\right) - \frac{\partial}{\partial z}\left(\frac{\partial F_1}{\partial T_z}\right) = 0 \quad \text{... (4.27)}$$

(within volume V)

$$\frac{\partial F_1}{\partial T_x} l_x + \frac{\partial F_1}{\partial T_y} l_y + \frac{\partial F_1}{\partial T_z} l_z + \frac{\partial F_2}{\partial T} = 0 \quad \text{... (4.28)}$$

(on surface boundary S)

Exercise 4.1: Show that in case of two parameters (say $\bar{u}, \bar{v}$) defined in the domain A and boundary L we obtain the Euler's equations as,

$$\left.\begin{aligned} \frac{\partial F_1}{\partial \bar{u}} - \frac{\partial}{\partial x}\left(\frac{\partial F_1}{\partial \bar{u}_x}\right) - \frac{\partial}{\partial y}\left(\frac{\partial F_1}{\partial \bar{u}_y}\right) = 0 \\ \frac{\partial F_1}{\partial \bar{v}} - \frac{\partial}{\partial x}\left(\frac{\partial F_1}{\partial \bar{v}_x}\right) - \frac{\partial}{\partial y}\left(\frac{\partial F_1}{\partial \bar{v}_y}\right) = 0 \end{aligned}\right\} \text{(in domain } A)$$

and

$$\left.\begin{aligned} \frac{\partial F_1}{\partial \bar{u}_x} l_x + \frac{\partial F_1}{\partial \bar{u}_y} l_y + \frac{\partial F_2}{\partial \bar{u}} = 0 \\ \frac{\partial F_1}{\partial \bar{v}_x} l_x + \frac{\partial F_1}{\partial \bar{v}_y} l_y + \frac{\partial F_2}{\partial \bar{v}} = 0 \end{aligned}\right\} \text{(on boundary } L)$$

Hint. Assume $\bar{\bar{u}} = \bar{u} + \varepsilon m$ and $\bar{\bar{v}} = \bar{v} + \varepsilon n$, where m and n are two independent functions of x, y.

4.3 STEADY-STATE ANALYSIS

Having established the essential conditions required to satisfy the governing equation and boundary conditions (Euler-Lagrange equations), we now proceed to apply it to steady state heat conduction problem governed by eq. 4.2 in the domain and eq. 4.3 at the boundary. Restating these,

$$k\left(\frac{\partial^2 T}{\partial x^2}+\frac{\partial^2 T}{\partial y^2}+\frac{\partial^2 T}{\partial z^2}\right)+\dot{Q}=0 \text{ in domain (volume) } V \quad \text{... (4.29)}$$

and,

$$T = T_0 \text{ on part of the surface boundary, } S_1$$

$$k\frac{\partial T}{\partial n}+\alpha T+q=0 \text{ on another part of the surface boundary, } S_2 \quad \text{...(4.30)}$$

where α and q are constants derived from the surface heat transfer coefficient and ambient temperature. The functionals for these equations are obtained as

$$F_1=\frac{1}{2}k\left[\left(\frac{\partial T}{\partial x}\right)^2+\left(\frac{\partial T}{\partial y}\right)^2+\left(\frac{\partial T}{\partial z}\right)^2\right]-\dot{Q}T \quad \text{... (4.31)}$$

$$F_2=\frac{1}{2}\alpha T^2+qT \quad \text{... (4.32)}$$

It is easy to see that substitution of these functionals in Euler-Lagrange eqs. (4.27, 4.28) give the governing equation and second boundary conditions for this problem (eqs. 4.29, 4.30). The first boundary condition will be satisfied using a special solution procedure (Chapter 3). Now our problem is well posed and its solution is equivalent to minimization of sum of integrals of F_1 in domain V and F_2 on boundary S_2. Thus

$$I=\int_V F_1 dV+\int_{S_2} F_2 dS \quad \text{... (4.33)}$$

The second boundary condition given in expression (4.30) is satisfied in a natural manner when the integral I in (4.33) is minimized. This is sometimes called the *natural* boundary condition. The condition of constant boundary temperature ($T = T_0$) is to be forced on the solution using special procedure and hence it is called the *forced* boundary condition.

4.3.1 Element Characteristics

If we consider a 3D tetrahedron element, the temperature is given by an expression similar to the one used for displacement. Thus

$$T=\sum_{i=1}^{4} N_i T_i=[N]\{T^e\} \quad \text{... (4.34)}$$

where $[N]$ is shape function, the four components of which, N_1, N_2, N_3 and N_4, are derived in Sec. 2.3.1. $\{T^e\}$ is the elemental temperature vector having four nodal temperatures as its components. We substitute this expression for T in eqs. (4.31) and (4.32) and also express the volume and surface integrals of eq. (4.33) as the sum over all the elements of volume and surface integrals taken over individual elements. Thus

$$I = \sum_{e=1}^{m}\int_{V^e}\frac{1}{2}k\left[\left(\frac{\partial}{\partial x}[N]\{T^e\}\right)^2+\left(\frac{\partial}{\partial y}[N]\{T^e\}\right)^2+\left(\frac{\partial}{\partial z}[N]\{T^e\}\right)^2\right]dV$$
$$-\sum_{e=1}^{m}\int_{V^e}\dot{Q}[N]\{T^e\}dV+\sum_{e=1}^{r}\int_{S^e}\frac{1}{2}\alpha([N]\{T^e\})^2\,dS$$
$$+\sum_{e=1}^{r}\int_{S^e}q[N]\{T^e\}dS \quad \text{... (4.35)}$$

where m and r represent the number of elements in the domain and on specified boundary respectively. Since this expression is the summation of terms over all the elements, we shall encounter values of temperature at all the nodes in the individual expressions for $\{T^e\}$. We also observe that terms such as shape function, thermal conductivity, $\alpha, q, \dot{Q}$ are either functions of coordinates or constants. Since these can be evaluated they are not unknowns. The only unknowns present in this expression for I are the nodal temperatures $T_1, T_2, \ldots T_n$. Extremization (or minimization here) of I implies that its partial derivatives with respect to $T_1, T_2, \ldots T_n$ be equated to zero. Thus

$$\frac{\partial I}{\partial T_1}=0$$
$$\frac{\partial I}{\partial T_2}=0$$
$$\vdots \quad \text{... (4.36)}$$
$$\frac{\partial I}{\partial T_n}=0$$

We now concentrate on finding the quantities expressed in eq. (4.36) for individual elements which can later be summed to get an overall expression. Again, we note that in the case of a tetrahedron element a single element will contribute to only four of the terms of eq. (4.36) because it contains only four nodal temperature values (say, T_1, T_2, T_3 and T_4). Thus for an element 'e' we obtain its contribution as

$$\left\{\frac{\partial I^e}{\partial\{T^e\}}\right\} = \begin{Bmatrix} \frac{\partial I^e}{\partial T_1} \\ \frac{\partial I^e}{\partial T_2} \\ \frac{\partial I^e}{\partial T_3} \\ \frac{\partial I^e}{\partial T_4} \end{Bmatrix} \quad \text{... (4.37)}$$

The expression for I^e is obtained from eq. (4.35) by considering a single element and we can write it as follows after differentiating within the integral sign

$$\frac{\partial I^e}{\partial T_1} =$$

$$\int_{V^e} k\left[\frac{\partial}{\partial x}[N]\{T^e\}\frac{\partial N_1}{\partial x} + \frac{\partial}{\partial y}[N]\{T^e\}\frac{\partial N_1}{\partial y} + \frac{\partial}{\partial z}[N]\{T^e\}\frac{\partial N_1}{\partial z}\right]dV^{(3)}$$

$$- \int_{V^e} \dot{Q}N_1\, dV + \int_{S^e} \alpha[N]\{T^e\}N_1\, dS + \int_{S^e} qN_1\, dS \quad \text{... (4.38)}$$

$$= \left(\frac{\partial I^e}{\partial T_1}\right)_A + \left(\frac{\partial I^e}{\partial T_1}\right)_B + \left(\frac{\partial I^e}{\partial T_1}\right)_C + \left(\frac{\partial I^e}{\partial T_1}\right)_D \quad \text{... (4.39)}$$

Since nodal temperatures behave as constants during integration over the volume of the element, these can be taken out of the integration as constants. Thus the first integral of expression (4.39) can be written as

[3] Note that,

$$\frac{\partial}{\partial T_1}\left(\frac{\partial}{\partial x}[N]\{T^e\}\right) = \frac{\partial}{\partial x}\left\{\frac{\partial}{\partial T_1}(N_1T_1 + N_2T_2 + N_3T_3 + N_4T_4)\right\} = \frac{\partial N_1}{\partial x}$$

$$\left(\frac{\partial I^e}{\partial T_1}\right)_A = \left\{\int_{V^e} k\frac{\partial N_1}{\partial x}\frac{\partial N_1}{\partial x}dV\right\}T_1 + \left\{\int_{V^e} k\frac{\partial N_1}{\partial x}\frac{\partial N_2}{\partial x}dV\right\}T_2$$

$$+ \left\{\int_{V^e} k\frac{\partial N_1}{\partial x}\frac{\partial N_3}{\partial x}dV\right\}T_3 + \left\{\int_{V^e} k\frac{\partial N_1}{\partial x}\frac{\partial N_4}{\partial x}dV\right\}T_4$$

$$+ \left\{\int_{V^e} k\frac{\partial N_1}{\partial y}\frac{\partial N_1}{\partial y}dV\right\}T_1 + \ldots$$

$$+ \left\{\int_{V^e} k\frac{\partial N_1}{\partial z}\frac{\partial N_1}{\partial z}dV\right\}T_1 + + \ldots \quad \text{... (4.40)}$$

$$= h_{11}^e T_1 + h_{12}^e T_2 + h_{13}^e T_3 + h_{14}^e T_4 \quad \text{... (4.41)}$$

where,

$$h_{1j}^e = \int_{V^e} k\left(\frac{\partial N_1}{\partial x}\frac{\partial N_j}{\partial x} + \frac{\partial N_1}{\partial y}\frac{\partial N_j}{\partial y} + \frac{\partial N_1}{\partial z}\frac{\partial N_j}{\partial z}\right)dV$$

$$= \int_{V^e} k\frac{\partial N_1}{\partial x_m}\frac{\partial N_j}{\partial x_m}dV$$ (using summation convention explained in Chapter 3; $m = 1, 2, 3$)

It is easy to see that similar expressions obtained after differentiating I^e with respect to T_2, T_3, T_4 will be,

$$\left(\frac{\partial I^e}{\partial T_2}\right)_A = h_{21}^e T_1 + h_{22}^e T_2 + h_{23}^e T_3 + h_{24}^e T_4 \text{ etc.}$$

Combining all such terms, part A of the elemental contributions becomes

$$\left(\frac{\partial I^e}{\partial\{T^e\}}\right)_A = \begin{Bmatrix} \frac{\partial I^e}{\partial T_1} \\ \frac{\partial I^e}{\partial T_2} \\ \frac{\partial I^e}{\partial T_3} \\ \frac{\partial I^e}{\partial T_4} \end{Bmatrix}_A = \begin{bmatrix} h_{11}^e & h_{12}^e & h_{13}^e & h_{14}^e \\ h_{21}^e & - & - & - \\ h_{31}^e & - & - & - \\ h_{41}^e & - & - & h_{44}^e \end{bmatrix} \begin{Bmatrix} T_1 \\ T_2 \\ T_3 \\ T_4 \end{Bmatrix} = [h^e]\{T^e\} \quad \text{... (4.42)}$$

where,

$$h_{ij}^e = \int_{V^e} k \frac{\partial N_i}{\partial x_m} \frac{\partial N_j}{\partial x_m} dV \qquad \text{... (4.43)}$$

Other terms of (4.39) are evaluated in a similar manner and these are obtained as

$$\left(\frac{\partial I^e}{\partial\{T^e\}}\right)_B = \{f_Q^e\} \text{ where } \underset{(i=1,2,3,4)}{f_{Qi}^e} = -\int_{V^e} \dot{Q} N_i \, dV$$

$$\left(\frac{\partial I^e}{\partial\{T^e\}}\right)_D = \{f_q^e\} \text{ where } \underset{(i=1,2,3,4)}{f_{qi}^e} = \int_{S^e} q N_i \, dS \qquad \text{... (4.44)}$$

$$\left(\frac{\partial I^e}{\partial\{T^e\}}\right)_C = [\overline{h^e}]\{T^e\} \text{ where } \underset{(i=1,2,3,4)}{\overline{h_{ij}^e}} = \int_{S^e} \alpha N_i N_j \, dS$$

On substituting in expression (4.37) we obtain the elemental contributions as

$$\left\{\frac{\partial I^e}{\partial\{T^e\}}\right\} = [h^e]\{T^e\} + [\overline{h^e}]\{T^e\} + \{f_Q^e\} + \{f_q^e\} \qquad \text{... (4.45)}$$

The elemental contributions are substituted in eq. (4.36) and this assembly results in the final matrix equation as

$$[H]\{T\} + [\overline{H}]\{T\} + \{f_Q\} + \{f_q\} = 0 \qquad \text{... (4.46)}$$

The terms of $[\overline{H}]$ matrix and $\{f_q\}$ vector are contributed from the elements located at the boundary. In symbolic notations we can represent these matrices as,

$$[H] = \sum_{e=1}^{m} [h^e] \quad ; \quad [\overline{H}] = \sum_{e=1}^{r} [\overline{h^e}]$$

$$[f_Q] = \sum_{e=1}^{m} \{f_Q^e\} \quad ; \quad [f_q] = \sum_{e=1}^{r} \{f_q^e\} \qquad \text{... (4.47)}$$

4.3.2 Solution

The matrix eq. (4.46) is presented in the standard form as

$$[A]\{T\} + \{F\} = 0 \qquad \text{... (4.48)}$$

We have already incorporated the second type of boundary condition (eq. 4.3) into the formulation. The first type of boundary condition is now satisfied by modifying eq. (4.48). The method explained in Chapter 3 is invoked and all the terms of rows and columns of matrix $[A]$, which correspond to nodes of specified temperature, are made zero while the corresponding diagonal term is made 1. Vector $\{F\}$ is also suitably modified. The resultant matrix equation is inverted and vector $\{T\}$ is obtained as the solution.

4.3.3 Two-Dimensional Analysis

Extension of this derivation to a two-dimensional case is straightforward. The final eq. (4.46) as well as the definition of elemental stiffness matrices remain the same (eqs. 4.42 and 4.44) except that the order of matrices $[h^e]$ and $[\overline{h^e}]$ now reduces to 3×3 for a 2D triangular element and derivatives in the z-direction are not present in the expression for h_{ij}^e (eq. 4.43) and 'm' varies as 1, 2.

4.3.4 Axi-Symmetric Case

The steady-state heat conduction equation for an axi-symmetric case, in which temperature does not vary in θ-direction and thermal conductivity is constant, is given by[4]

$$k\left[\frac{\partial^2 T}{\partial r^2} + \frac{1}{r}\frac{\partial T}{\partial r} + \frac{\partial^2 T}{\partial z^2}\right] + \dot{Q} = 0 \qquad \text{... (4.49)}$$

The Euler-Lagrange equation for an axi-symmetric case can be obtained using the procedure explained in Sec. 4.2.2; its form is given as[5]

---

[4] The general expression, when k is temperature dependent and shows anisotropy in r and z direction, is

$$\frac{k_r}{r}\frac{\partial T}{\partial r} + \frac{\partial}{\partial r}\left(k_r \frac{\partial T}{\partial r}\right) + \frac{\partial}{\partial z}\left(k_z \frac{\partial T}{\partial z}\right) + \dot{Q} = 0.$$

[5] The term such as the one given in eq. (4.20) will now be,

$$\int_V \frac{\partial F_1}{\partial T_r}\frac{\partial n}{\partial r} dV = \int_z \int_r \frac{\partial F_1}{\partial T_r}\frac{\partial n}{\partial r} 2\pi r \, dr \, dz.$$

On integration by parts it gives,

$$2\pi \int_z \left[nr \frac{\partial F_1}{\partial T_r}\Big|_0^r - \int_r n \frac{\partial}{\partial r}\left(r \frac{\partial F_1}{\partial T_r}\right) dr \right] dz.$$

Substituting for dz as $l_r \cdot dL$ in the first term, we obtain,

$$\int_L n \frac{\partial F_1}{\partial T_r} l_r \, 2\pi r \, dL - \int_z \int_r n \frac{1}{r}\frac{\partial}{\partial r}\left(r \frac{\partial F_1}{\partial T_r}\right) 2\pi r \, dr \, dz.$$

The first term contributes to the boundary integral while the second term gives the two terms of the first equation of expression (4.50).

$$\frac{\partial F_1}{\partial T} - \frac{1}{r}\frac{\partial F_1}{\partial T_r} - \frac{\partial}{\partial r}\left(\frac{\partial F_1}{\partial T_r}\right) - \frac{\partial}{\partial z}\left(\frac{\partial F_1}{\partial T_z}\right) = 0 \text{ (in volume } V\text{)}$$

and

$$\frac{\partial F_1}{\partial T_r} l_r + \frac{\partial F_1}{\partial T_z} l_z + \frac{\partial F_2}{\partial T} = 0 \text{ (on boundary } S\text{)} \quad \text{... (4.50)}$$

The functional F_1 and F_2 now have the form

$$F_1 = k\left[\left(\frac{\partial T}{\partial r}\right)^2 + \left(\frac{\partial T}{\partial z}\right)^2\right] - \dot{Q}T$$

$$F_2 = \frac{1}{2}\alpha T^2 + qT \quad \text{... (4.51)}$$

Substitution of these expressions for functionals in eq. (4.50) yields the governing eq. (4.49) in the domain and the boundary condition (from eq. 4.30) at axi-symmetric boundary S_2.

The finite element formulation beyond this stage follows the procedure of 3D analysis explained in Sec. 4.3.1 and the elemental matrices $[h^e]$, $[\overline{h^e}]$ and vectors $\{f_Q^e\}$ and $\{f_q^e\}$ have expressions similar to those in eqs. (4.42) to (4.44). Thus

$$h_{ij}^e = \int_z \int_r k\left(\frac{\partial N_i}{\partial r}\frac{\partial N_j}{\partial r} + \frac{\partial N_i}{\partial z}\frac{\partial N_j}{\partial z}\right) 2\pi r\, dr\, dz$$

$$f_{Qi}^e = -\int_z \int_r \dot{Q} N_i\, 2\pi r\, dr\, dz$$

$$f_{qi}^e = \int_{L^e} q N_i\, 2\pi r\, dL \quad \text{... (4.52)}$$

$$\overline{h_{ij}^e} = \int_{L^e} \alpha N_i N_j\, 2\pi r\, dL$$

The final matrix relation is again obtained as

$$[H]\{T\} + [\overline{H}]\{T\} + \{f_Q\} + \{f_q\} = 0$$

where the matrices and vectors are given by eq. (4.47). The constant temperature boundary condition can be enforced by modifying the matrix and the solution for temperature is obtained as explained in Sec. 4.3.2. The evaluation of various terms of (4.52) is performed using numerical integration (see Chapters 2 and 7).

4.4 ILLUSTRATIVE EXAMPLES

4.4.1 Cutting Tool

Study of temperature rise in cutting tool during metal cutting (turning) has attracted the attention of investigators due to the influence of temperature rise on tool life. The results of such two-dimensional analysis of the temperature field in a cutting tool are presented here. The model assumed heat input at a point located close to the tool tip where the chip rubs against the tool face. The end face of the tool, far away from the tip, is assumed to remain at room temperature at the location where it is held in the tool holder. Other surfaces are taken to be adiabatic. In practice, the tool attains a steady-state temperature distribution in a few minutes. The simplified model explained above was analyzed using a two-dimensional finite element model. Linear triangular elements were used. Fine grid was used close to the tip where the temperature gradients were expected to be very steep. The grid and the resultant temperature isotherms are shown in Fig. 4.5.

The analysis was performed on a high-speed steel (H.S.S) tool. The mild steel workpiece was turned at cutting speed of 45 m/min. For metal removal rate of 11.25 cm^3/min and specific unit power of 37×10^{-3} kW/cm^2/min, the cutting power was obtained as 416 W. Temperature distribution in the tool was determined by considering that 10% of this power was used for heating the tool of 10 mm thickness. Thermal conductivity of the tool material (H.S.S) was taken as 24.1 W/mK. The fine mesh used at the tool tip was able to capture the steep temperature gradients. The boundary conditions represented by symbol Δ imply constant temperature (30°) along that edge. ANSYS[6] finite element package was used for this analysis. The example shows that even simple two-dimensional steady-state analysis was capable of predicting temperature distribution reasonably well in this case.

4.4.2 Continuously Cast Steel Billet

This illustrates another important practical application of the thermal finite element model reported by Kelly et al. [1]. The molten steel from the melting furnace flows into a tundish from where it flows out through a mould in the form of a long strand as shown in Fig. 4.6. As this strand (or billet) comes out of the mould it starts to solidify at the skin, thus carrying the molten metal within it which also solidifies later. This hot billet is sent directly to the rolling mill to avoid the costly reheating operation necessary when steel has solidified in an ingot mould. Rupture of the solidified skin

[6] ANSYS is the registered trademark of Swanson Analysis System, Inc.

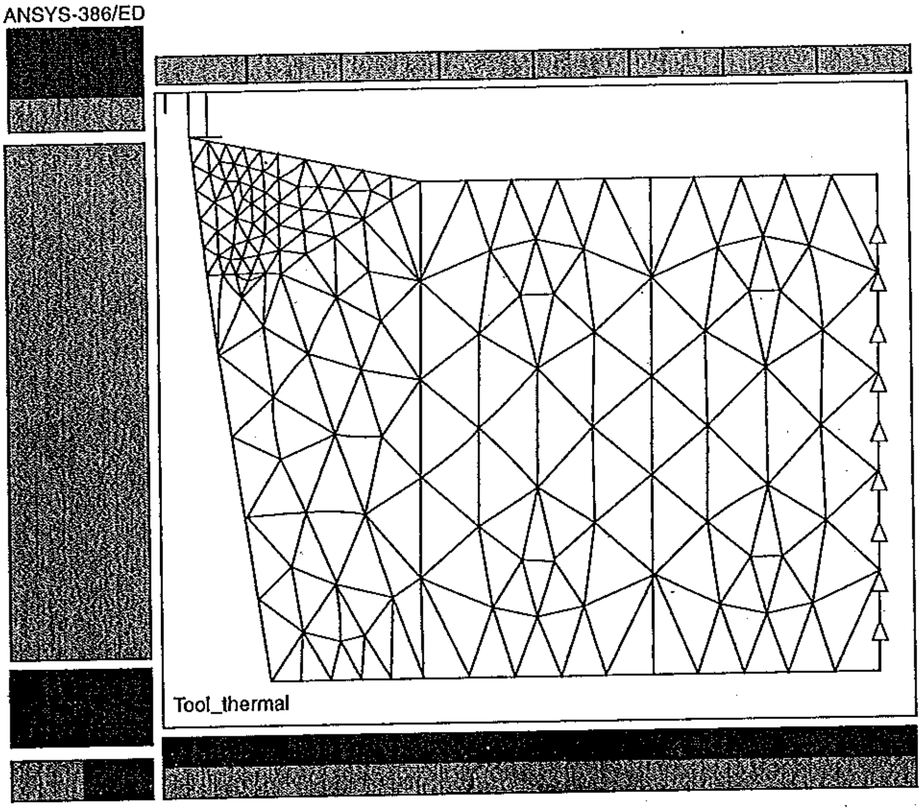

(a): Grid used.

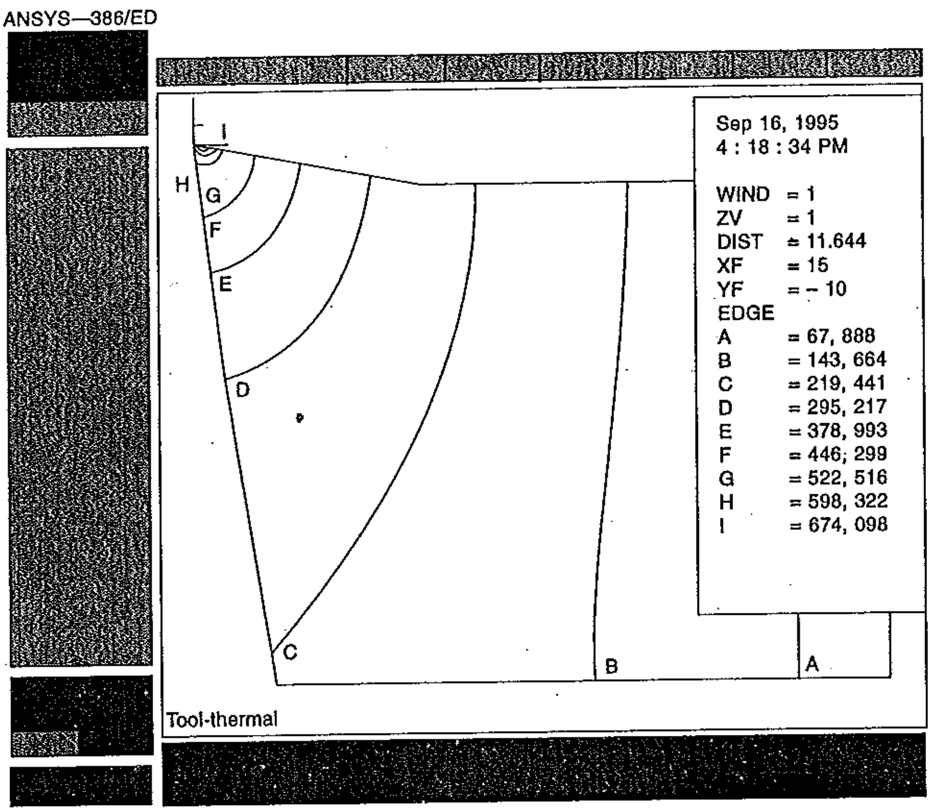

(b) Temperature distribution

Fig. 4.5 Steady state heat conduction analysis in a turning tool.

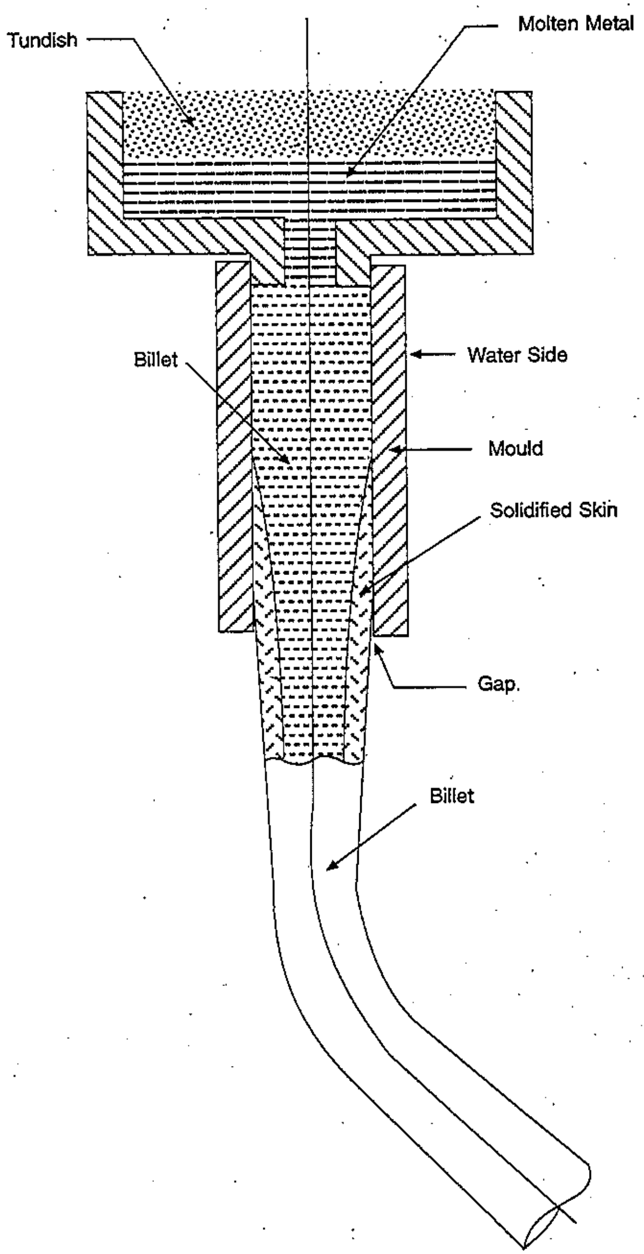

Fig. 4.6: Continuous casting of steel billet.

of the billet under the pressure of the molten metal at the instant the billet emerges from the mould is a major problem in this continuous casting operation. To tackle this, the complete sequence of heat transfer from billet to mould and from mould to the surrounding atmosphere or cooling water spray, should be analyzed. The various factors considered by Kelly are:

(i) Fluid flow from tundish to billet analyzed in order to obtain velocity distribution.
(ii) Convective-conductive heat flow into mould-billet system analyzed using the velocity distribution obtained in step (i). Heat transfer coefficients at various surfaces taken from the literature or assumed initially.
(iii) Temperature distribution in the billet, obtained in step (ii) used to determine billet shrinkage and the gap created between the mould and billet.
(iv) Heat transfer coefficient further modified depending on the magnitude of the gap and on the basis of conductivity of gases in this gap.
(v) Steps (ii) to (iv) performed again and these iterations continued until converged solution of temperature distribution obtained.

At all these stages the latent heat of solidification, variation of thermal conductivity with temperature and any variation in heat transfer coefficient were considered. Finally, stress analysis was performed to determine the cracking tendency of the solidified skin. The cooling rate calculated during various stages of solidification and subsequent cooling was used to estimate the microstructure.

4.4.3 Auto-Engine Analysis and Design

The performance simulation of an automobile engine is also done through a thermal model. Smith et al. [5] have reported such a study. Thermal analysis involves an engine cylinder block and head, valves and piston as well as the combustion chamber. The combustion process is simulated using a numerical software. Computational fluid dynamics (CFD) analysis is used to study flow through the cooling passages in the engine cylinder block and head. The surface heat transfer coefficients and temperatures calculated in the fluids (coolants or combustion products) are used to analyze temperature distribution in the cylinder block, head and piston by applying conductive finite element analysis. Even the boiling heat transfer in some regions of the system is taken into account. Iterative correction of these heat transfer parameters is carried out until convergence is obtained.

The work of Smith et al. also reports the use of a stress-analysis finite element program for mechanical design and optimization of engine components such as crankshaft, connecting rod, cylinder block etc., which is integrated with thermal analysis.

4.5 HEAT-TRANSFER COEFFICIENT

The importance of the heat-transfer coefficient at the solid-gas contact interfaces or solid-water contact surface is highlighted in the above examples. The values of these heat-transfer coefficients vary widely depending the nature and orientation of the surface (i.e., horizontal or vertical), flow velocity of gas or liquid over the surface, constriction of gas due to narrow gaps and so on. This coefficient may also vary from point to point on the surface and an iterative correction of the same may be necessary during the analysis based on the surface temperature and other conditions prevailing at the particular instant. It is essential to use the appropriate heat-transfer coefficient in the thermal analysis without which the results will be highly erroneous. Extensive information on the magnitude of this coefficient under different conditions is available in texts on heat transfer[6] which should be consulted before performing a thermal finite element analysis.

REFERENCES

1. Kelly, J.E., Michalek, K.P., O'connor, T.G., Thomas, B.G. and Dantzig, J.A. 1988. Initial development of thermal and stress fields in continuously cast steel billets, *Met. Trans.* A, .19A: p 2589–2602.
2. Pillinger, I., Hartley, P., Sturgess, C.E.N. and Rowe, G.W. 1988. Finite element modelling of metal flow in three-dimensional forming. *Int. J. Num. Meth. Engg.*, 25: p 87–97.
3. Gupta, O.P., Dorn, L. and De, Amitava 1994. An evaluation of resistance spot welding process of low carbon steel and HSLA steel sheets. Proc. National Welding Seminar, Ind. Inst. of Welding, Jamshedpur, p. 6x1/5–9.
4. Reddy, J.N. and Rasmussen, M.L. 1982. *Advanced Engineering Analysis*, John Wiley and Sons, N.Y.
5. Smith, A.V., Johns, R.J.R. and McNamara, P.M. 1994. Improving the process of engine design through the integrated application of CAE Methods. *Proc. Instn. Mech. Engrs.*, 208: p 259–267.
6. Holman, J.P. (1989). *Heat Transfer*, McGraw-Hill Book Co., N.Y. pp. 237–256, 323–360.

Chapter 5

WEIGHTED RESIDUE TECHNIQUE AND UNSTEADY-STATE HEAT-FLOW ANALYSIS

5.1 INTRODUCTION

The variational approach discussed in the previous chapter requires that a functional be obtained such that its minimization within the domain of analysis becomes equivalent to solving the governing equation of the problem. Euler-Lagrange equations form the basis of such a formulation. It is not easy to find such a functional. In fact, an appropriate functional may not always exist. We shall discuss here another technique which eliminates use of a functional as it works directly from the governing equation. The weighted residue technique, as it is called, is a very powerful method of finite element formulation. Although we shall use it in this chapter for unsteady-state heat-flow analysis, its strength will be demonstrated in subsequent chapters where it will be used for other applications.

The unsteady-state heat-flow analysis which forms the topic of this chapter has many important engineering applications. In fact, several examples given initially in Chapter 4 fall in this category. Heating an object in a furnace, temperature distribution in resistance welding or heating of forging dies are such examples. In these cases the temperature field keeps on changing with time and never attains a steady state. There are many engineering applications in which an unsteady state of temperature field prevails. Heating of a rocket nozzle and casing after take-off, combustion inside an auto-engine cylinder and subsequent heating of the cylinder, solidification and cooling of castings, rapid heating and cooling in arc welding, laser cutting, cooling of ingots in steel processing, cooling during hardening heat treatment etc. are examples of unsteady-state heat flow. Some of these are depicted in Fig. 5.1.

Knowledge of the temperature field is directly useful in some cases, such as welding, laser cutting, heat treatment or cooling of castings in which the cooling rate plays a very important role in development of desirable or undesirable metallurgical microstructure. Hard, brittle microstructure may result in crack formation. In other cases a rapid temperature gradient results in severe thermal stresses and subsequent

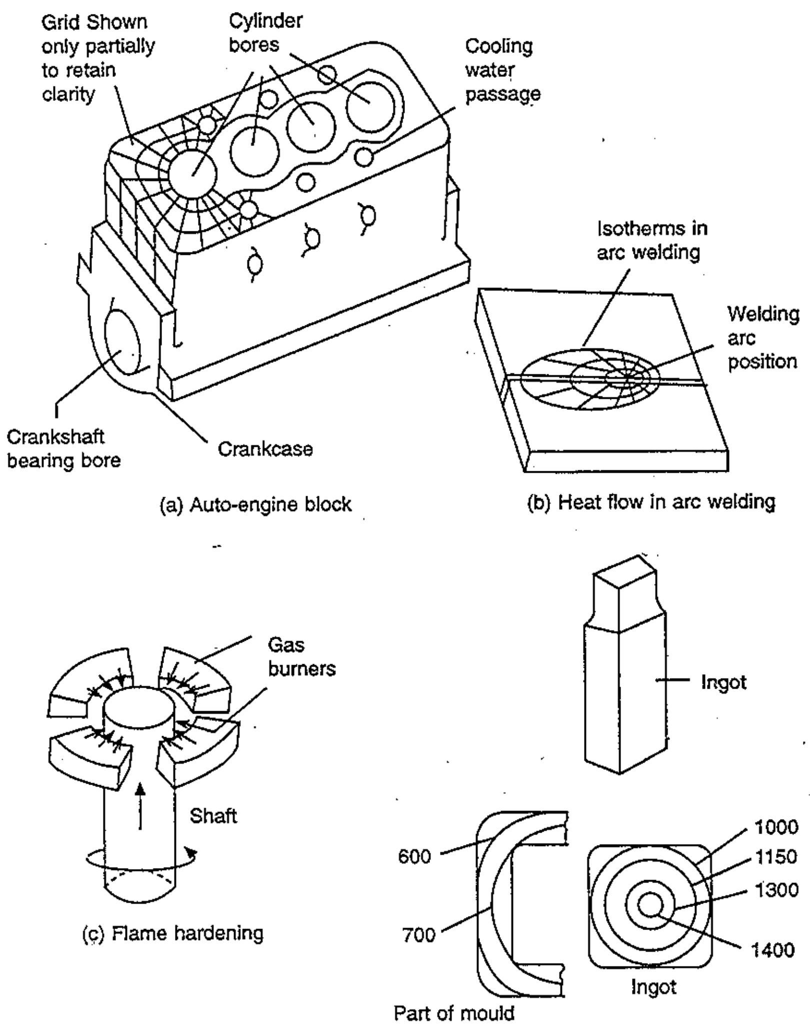

(a) Auto-engine block

(b) Heat flow in arc welding

(c) Flame hardening

(d) Isotherms along cross-section of an ingot-mould system in steel melting shop

Fig. 5.1 Applications of unsteady-state heat-flow analysis.

failure. In a combustion chamber thermal analysis may help in identifying hot spots for subsequent placement of the fuel spray nozzle in a most advantageous manner. Thermal analysis coupled with fluid-flow analysis provides very useful information about surface heating during very high speed flow, such as occurs in the re-entry of a space shuttle into the atmosphere.

5.2 WEIGHTED RESIDUE TECHNIQUE

Suppose the governing equation and boundary conditions to be satisfied by a solution are written in symbolic form as
Governing eq.:

$$A(T) = 0 \qquad \text{... (5.1)}$$

Boundary condition:

$$B(T) = 0$$

If we assume an arbitrary temperature distribution in the domain, say T', and substitute it in eq. (5.1), these equations will not be satisfied; we shall obtain

$$A(T') = R_1 \neq 0$$
$$B(T') = R_2 \neq 0 \qquad \text{... (5.2)}$$

The quantities R_1 and R_2 are called residues. The residue left by equation $A(T')$ will differ at different points in the domain such as 1, 2, 3... in Fig. 5.2. The residue left by boundary condition $B(T')$ will likewise differ at various boundary points. For T' to be the solution of the governing equation under the given boundary condition, these residues should be zero at all the points within the domain and on the boundary. We may think of a procedure by which this can be ensured. Consider a one-dimensional domain extending from point A to B as shown in Fig. 5.3. If the distribution of residue for some arbitrary temperature distribution T' is given by $A(T')$ as shown in the Figure and if we consider another arbitrary function w and multiply $A(T')$ by w at every point and add these products, we obtain the quantity

$$\int_A^B w \cdot A(T')\, dx$$

Since w is an arbitrary function and $A(T')$ will not be zero at all the points for a distribution T' which is not the solution of the problem, there is little likelihood that the integral expressed above will be zero. Again, if we consider several arbitrary distributions of w (say $w_1, w_2...$) and obtain a distribution of T which makes this integral zero for all values of w, then the only possibility in which this can happen is when T is the desired solution of the problem. This logic forms the basis of the weighted residue approach and functions w are known as weighting functions. Thus the condition for a temperature distribution T to be the solution of a problem stated in the form of expression (5.1) is

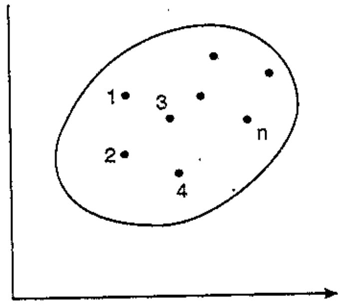

Fig. 5.2

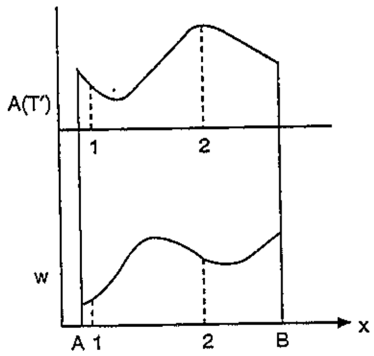

Fig. 5.3 Residue and weighting functions

$$\int_V w_1 A(T)\, dv + \int_S w_2 B(T)\, dS = 0^{(1)} \qquad \text{... (5.3)}$$

where w_1, w_2 comprise many sets of arbitrary weighting functions.

5.2.1 Form of Weighting Function

Although the weighting function can be totally arbitrary, it should satisfy a few requirements in order to be useful in finite element implementation. First, all such functions should be totally independent. Secondly, the functions should be simple in order to avoid computational difficulties. With this objective we look at the following function. Consider a one-dimensional object, shown in Fig. 5.4, which is divided into elements 1-2, 2-3, ... and thus has n nodes. We have already discussed the concept of nodal shape functions N_1, N_2... in Chapter 2. A nodal shape function has relevance to a particular node and adjoining elements only. Also it has a value 1 at the particular node and its value drops to zero as we approach the other nodes of adjoining elements. For a linear shape function the variation of N from one node to another is also linear. Thus, if we consider node 3 in Fig. 5.4, function N_3 has value 1 at this node while its value drops to zero at the other nodes of adjoining elements (nodes 2 and 4). In the rest of the domain N_3 has no meaning and its value there is taken as zero. The Figure also shows the distribution of N_6 by a broken line. It can be seen that the two distributions of shape functions show no relation to each other. It is easy to visualize that there will be 'n' such independent distributions of shape functions, N_is. These shape functions can be used

[1]There are some other forms of weighted residue statements such as least square statement or point collocation method. However, the statement expressed by eq. (5.3) is the most common form.

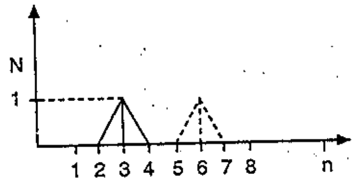

Fig. 5.4 Variations of nodal shape functions

as weighting functions and this approach to selecting weighting functions is called the Galerkin process. For convenience we take w_1 as N_i and w_2 as $-N_i (i = 1, 2, \dots n)$. The weighted residue statement now becomes

$$\int_V N_i A(T)\, dv - \int_S N_i B(T)\, dS = 0 \qquad \text{... (5.4)}$$

5.3 APPLICATION TO STEADY-STATE HEAT FLOW

We first apply the weighted residue technique to formulation of the steady-state heat-flow problem discussed in Chapter 4 and compare the two results. Using the governing equation, $A(T)$, and boundary condition, $B(T)$, given in eqs. (4.2) and (4.3), we obtain the weighted residue statement as

$$\int_V N_i \left[k \left(\frac{\partial^2 T}{\partial x^2} + \frac{\partial^2 T}{\partial y^2} + \frac{\partial^2 T}{\partial z^2} \right) + \dot{Q} \right] dV -$$

$$- \int_S N_i \left[k \frac{\partial T}{\partial n} + \alpha T + \dot{q} \right] dS = 0 \qquad \text{... (5.5)}$$

or

$$\int_V k N_i \nabla^2 T\, dV + \int_V N_i \dot{Q}\, dV - \int_S k N_i \frac{\partial T}{\partial n} dS -$$

$$- \int_S N_i\, \alpha T\, dS - \int_S N_i q\, dS = 0 \qquad \text{... (5.6)}$$

Using the first form of Green's theorem (eq. 3.37) to rewrite the first term of eq. (5.6), we obtain

$$- \int_V k \left(\frac{\partial N_i}{\partial x} \frac{\partial T}{\partial x} + \frac{\partial N_i}{\partial y} \frac{\partial T}{\partial y} + \frac{\partial N_i}{\partial z} \frac{\partial T}{\partial z} \right) dV + \int_S k N_i \frac{\partial T}{\partial n} dS +$$

$$+ \int_V N_i \dot{Q}\, dV - \int_S k N_i \frac{\partial T}{\partial n} dS - \int_S N_i \alpha T dS - \int_S N_i q dS = 0 \qquad \text{... (5.7)}$$

or

$$\int_V k\left(\frac{\partial N_i}{\partial x}\frac{\partial T}{\partial x}+\frac{\partial N_i}{\partial y}\frac{\partial T}{\partial y}+\frac{\partial N_i}{\partial z}\frac{\partial T}{\partial z}\right)dV-\int_V N_i\dot{Q}\,dV+$$
$$+\int_S N_i\alpha T\,dS+\int_S N_i q\,dS=0 \qquad \ldots (5.8)$$

On discretizing the domain into four-noded tetrahedron elements, the temperature within the element can be expressed in terms of nodal temperature as

$$T=\sum_{i=1}^{4} N_i T_i=[N]\{T^e\} \qquad \ldots (5.9)$$

The volume integrals and surface integrals shown in eq. (5.8) are expressed as the sum over all the elements of the respective integrals performed within the elements. If there exist n nodes within the volume there will now be n unknown temperatures T_i in eq. (5.8). We need n such equations which can be solved simultaneously to obtain these T_i. These equations are easily obtained by considering n separate values of weight functions, N_i, each giving one equation. Since there exist n nodes we have as many values of N_i available with us. Eq. (5.8) can now be expressed as a set on n equations as follows

$$\sum_{e=1}^{m}\int_{V^e} k\left(\frac{\partial N_i}{\partial x}\frac{\partial T}{\partial x}+\frac{\partial N_i}{\partial y}\frac{\partial T}{\partial y}+\frac{\partial N_i}{\partial z}\frac{\partial T}{\partial z}\right)dV-\sum_{e=1}^{m}\int_{V^e} N_i\dot{Q}\,dV+$$
$$+\sum_{e=1}^{r}\int_{S^e} N_i\alpha T\,dS+\sum_{e=1}^{r}\int_{S^e} N_i q\,dS=0 \qquad \ldots (5.10)$$

where, as usual, we have m elements, of which r elements have boundary of domain as their face. Since there exist only four nodes in a tetrahedron element, there will exist only four non-zero values of N_i for an element. Thus an element will contribute terms only in four equations of a set of n equations expressed as (5.10) (i.e., eqs. related to relevant N_i values). If four nodes associated with an element 'e' are designated as 1, 2, 3, 4 for simplicity, the corresponding termwise contribution from this element towards eq. set (5.10) will be:

(i) For first term

$$\int_{V^e} k\left(\frac{\partial N_1}{\partial x}\frac{\partial [N]}{\partial x}\{T^e\}+\frac{\partial N_1}{\partial y}\frac{\partial [N]}{\partial y}\{T^e\}+\frac{\partial N_1}{\partial z}\frac{\partial [N]}{\partial z}\{T^e\}\right)dV$$

$$\int_{V^e} k\left(\frac{\partial N_2}{\partial x}\frac{\partial [N]}{\partial x}\{T^e\}+\frac{\partial N_2}{\partial y}\frac{\partial [N]}{\partial y}\{T^e\}+\frac{\partial N_2}{\partial z}\frac{\partial [N]}{\partial z}\{T^e\}\right)dV$$

$$\int_{V^e} k\left(\frac{\partial N_4}{\partial x}\frac{\partial [N]}{\partial x}\{T^e\}+\frac{\partial N_4}{\partial y}\frac{\partial [N]}{\partial y}\{T^e\}+\frac{\partial N_4}{\partial z}\frac{\partial [N]}{\partial z}\{T^e\}\right)dV \qquad \ldots (5.11)$$

Since terms of $\{T^e\}$ are nodal temperatures which do not vary within the element, this vector can be taken out of the integral sign and on rearranging the rest of the terms we obtain this elemental contribution in matrix form as

$$\begin{bmatrix} h_{11}^e & h_{12}^e & h_{13}^e & h_{14}^e \\ h_{21}^e & h_{22}^e & h_{23}^e & h_{24}^e \\ h_{31}^e & h_{32}^e & h_{33}^e & h_{34}^e \\ h_{41}^e & h_{42}^e & h_{43}^e & h_{44}^e \end{bmatrix}\begin{Bmatrix} T_1 \\ T_2 \\ T_3 \\ T_4 \end{Bmatrix}=[h^e]\{T^e\} \qquad \ldots (5.12)$$

where

$$h_{ij}^e=\int_{V^e} k\frac{\partial N_i}{\partial x_m}\frac{\partial N_j}{\partial x_m}dV$$

(using summation convention; see eq. 4.41)

(ii) For 2nd term

The element contribution towards the second term is made of four terms given as

$$\underset{i=1,2,3,4}{f_{Qi}^e}=-\int_{V^e}\dot{Q}N_i\,dV \text{ or vector } \{f_Q^e\} \qquad \ldots (5.13)$$

(iii) For 3rd and 4th terms

The contributions towards the 3rd and 4th terms can similarly be obtained as

$$[\bar{h}^e]\{T^e\} \text{ and } \{f_q^e\}$$

where

$$\underset{(i,j=1,\cdots,4)}{\bar{h}_{ij}^e=\int_{S^e}\alpha N_i N_j\,dS} \quad \underset{(i=1,\cdots,4)}{f_{qi}^e=\int_{S^e} qN_i\,dS}$$

The total contribution from an element 'e' is thus obtained as,

$$[h^e]\{T^e\}+[\bar{h}^e]\{T^e\}+\{f_Q^e\}+\{f_q^e\} \qquad \ldots (5.14)$$

This is the same as that obtained in Chapter 4 as eq. (4.45). The final assembled matrix equation is now given by eq. (4.46).

We thus observe that the finite element matrix relation obtained by using the weighted residue technique with the Galerkin process is the same as obtained using the variational approach.

5.4 UNSTEADY-STATE HEAT FLOW

The transient heat conduction equation for a stationary solid is given by eq. (4.1) in which the velocity term is absent, i.e.

$$k\left[\frac{\partial^2 T}{\partial x^2}+\frac{\partial^2 T}{\partial y^2}+\frac{\partial^2 T}{\partial z^2}\right]+\dot{Q}=c\rho\frac{\partial T}{\partial \tau} \qquad \dots (5.15)$$

For this problem the initial condition should be specified which may be in the form of known temperature in the whole domain at time instant $\tau = 0$. Also the boundary condition at any instant is specified as either known temperature or known temperature gradient at part or whole of the boundary.
Thus

$$T = T_0 \text{ at } S_1 \quad \text{for} \quad \tau > 0$$

$$k\frac{\partial T}{\partial n}+\alpha T+q=0 \text{ at } S_2 \quad \text{for} \quad \tau > 0 \qquad \dots (5.16)$$

This boundary condition is the same as the one specified for the steady-state case. The weighted residue statement is again written as

$$\int_0^{\Delta\tau}\int_V w_1\left[k\left(\frac{\partial^2 T}{\partial x^2}+\frac{\partial^2 T}{\partial y^2}+\frac{\partial^2 T}{\partial z^2}\right)+\left(\dot{Q}-c\rho\frac{\partial T}{\partial \tau}\right)\right]dV\,d\tau$$

$$+\int_0^{\Delta\tau}\int_S w_2\left[k\frac{\partial T}{\partial n}+\alpha T+q\right]dS\,d\tau=0 \qquad \dots (5.17)$$

The integral has been taken over the volume (and surface) as well as time because our domain of analysis extends both in space and time. With the same logic the weighting functions w_1 and w_2 should also be functions of space and time. For simplicity we consider the time domain to extend over a single time step only. This means that if we consider the one-dimensional object shown in Fig. 5.5 with nodes 1, 2, ... n, then the temperatures at the beginning (time $\tau = 0$) are given as $T_1^1, T_2^1, \dots$ at various nodes while those at the end of time τ_2 are $T_1^2, T_2^2, T_3^2 \dots$ at these nodes. The temperature at any intermediate time instant can be written as

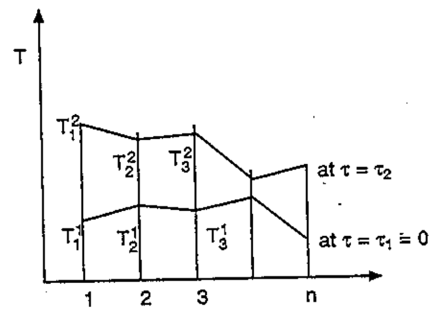

Fig. 5.5 Nodal temperature change with time

$$(T)_{node1} = N_{\tau_1}T_1^1 + N_{\tau_2}T_1^2$$

$$(T)_{node2} = N_{\tau_1}T_2^1 + N_{\tau_2}T_2^2 \qquad \dots (5.18)$$

$$\text{-------------}$$

where $N_{\tau 1}$, $N_{\tau 2}$ are the shape functions in the time domain. We now consider a weighting function which is the product of shape functions in space and time, i.e.

$$w_1 = N_\tau \cdot N_i$$

and

$$w_2 = -w_1 = -N_\tau \cdot N_i \qquad \dots (5.19)$$

Here N_τ symbolically represents $N_{\tau 1}$ or $N_{\tau 2}$. Note that this weighting function is now a function of space and time as envisaged in eq. (5.17). Also our domain is such that all the temperatures at initial instant of time τ_1 (= 0) are known (specified initial condition) and the only unknowns of the problem are 'n' temperatures at the nodes at the time instant τ_2. This requires only n equations and n weighting functions for solution. These n values of $N_\tau \cdot N_i$ ($i = 1, \dots n$) are obtained by taking a single value of N_τ ($N_{\tau 1}$ or $N_{\tau 2}$) and n values of N_i. We take N_τ as $N_{\tau 2}$ because the temperatures at the 2nd instant of time are to be determined. Thus knowing that $N_{\tau 2}$ is the function of time only eq. (5.17) becomes

$$\int_0^{\Delta\tau} N_{\tau 2}\left[\int_V N_i\left\{k\left(\frac{\partial^2 T}{\partial x^2}+\frac{\partial^2 T}{\partial y^2}+\frac{\partial^2 T}{\partial z^2}\right)+\left(\dot{Q}-c\rho\frac{\partial T}{\partial \tau}\right)\right\}dV\right.$$

$$\left.-\int_S N_i\left(k\frac{\partial T}{\partial n}+\alpha T+q\right)dS\right]d\tau=0 \qquad \dots (5.20)$$

The bracketed quantity can be evaluated in a manner similar to steady-state analysis of Sec. 5.3 except that an additional term $\int_V N_i \rho c \frac{\partial T}{\partial \tau}dV$ appears here. This term can be evaluated as follows

$$\int_V N_i \rho c \frac{\partial T}{\partial \tau} dV = \sum_{e=1}^{m} \int_{V^e} N_i \rho c \frac{\partial([N]\{T^e\})}{\partial \tau} dV \qquad \dots (5.21)$$

As discussed in Sec. 5.3, the elemental contribution given by eq. (5.21) appears in only four equations which have those values of N_i that appear in the element under consideration (say N_1, N_2, N_3, N_4). Thus the elemental contribution will comprise

$$\int_{V^e} N_1 \rho c [N] \, dV \frac{\partial \{T^e\}}{\partial \tau}$$

$$\int_{V^e} N_2 \rho c [N] \, dV \frac{\partial \{T^e\}}{\partial \tau} \qquad \dots (5.22)$$

$$\text{-------------}$$

$$\int_{V^e} N_4 \rho c [N] \, dV \frac{\partial \{T^e\}}{\partial \tau}$$

which can be written in matrix form as

$$[C^e] \frac{\partial \{T^e\}}{\partial \tau} \qquad \dots (5.23)$$

where

$$c_{ij}^e = \int_{V^e} \rho c N_i N_j \, dV \qquad \dots (5.24)$$
$$(i, j = 1, 2, 3, 4)$$

The net elemental contribution, i.e., eq. (5.14), now becomes

$$[h^e]\{T^e\} + [\bar{h}^e]\{T^e\} + [C^e] \frac{\partial \{T^e\}}{\partial \tau} + \{f_Q^e\} + \{f_q^e\} \qquad \dots (5.25)$$

When assembled in the form of contributions from all the elements of volume it becomes

$$[H]\{T\} + [\bar{H}]\{T\} + [C] \frac{\partial \{T\}}{\partial \tau} + \{f_Q\} + \{f_q\} \qquad \dots (5.26)$$

Substituting in eq. (5.20), we obtain

$$\int_0^{\Delta\tau} N_{\tau 2} \left[[H']\{T\} + [C] \frac{\partial \{T\}}{\partial \tau} + \{f\} \right] d\tau = 0 \qquad \dots (5.27)$$

where

$$[H'] = [H] + [\bar{H}] \text{ and } \{f\} = \{f_Q\} + \{f_q\}$$

The vector $\{T\}$ in expression (5.27) is nodal temperature vector having 'n' components, each one of which represents the temperature at a particular node at some instant of time τ in-between $\tau = \tau_1 = 0$ and $\tau = \tau_2$.

5.4.1 Shape Function in Time Domain

Referring back to Fig. 5.5 the temperatures at nodes 1, 2 are T_1^1, T_2^1 at the start of the time step, which change to T_1^2, T_2^2 at the end of time step τ_2. The only manner in which we can unambiguously specify the temperature at any intermediate time instant is to take a linear variation within these two temperature values. These temperatures at time instant τ are given as

$$T_1 = \left(\frac{\tau_2 - \tau}{\tau_2 - \tau_1}\right) T_1^1 + \left(\frac{\tau - \tau_1}{\tau_2 - \tau_1}\right) T_1^2 \quad \text{for node 1}$$

$$T_2 = \left(\frac{\tau_2 - \tau}{\tau_2 - \tau_1}\right) T_2^1 + \left(\frac{\tau - \tau_1}{\tau_2 - \tau_1}\right) T_2^2 \quad \text{for node 2} \qquad \dots (5.28)$$

$$\text{-------------}$$

or on representing the temperature values at all the nodes in vector form

$$\{T\} = \begin{Bmatrix} T_1 \\ T_2 \\ \cdot \\ \cdot \\ \cdot \\ T_n \end{Bmatrix}; \{T^1\} = \begin{Bmatrix} T_1^1 \\ T_2^1 \\ \cdot \\ \cdot \\ \cdot \\ T_n^1 \end{Bmatrix}; \{T^2\} = \begin{Bmatrix} T_1^2 \\ T_2^2 \\ \cdot \\ \cdot \\ \cdot \\ T_n^2 \end{Bmatrix} \qquad \dots (5.29)$$

where $\{T^1\}$ $\{T\}$ and $\{T^2\}$ are the temperature vectors at the start of the time step, at an intermediate time and at the end of the time step respectively. Thus on substituting in expression (5.28), we obtain

$$\{T\} = \left(\frac{\tau_2 - \tau}{\tau_2 - \tau_1}\right) \{T^1\} + \left(\frac{\tau - \tau_1}{\tau_2 - \tau_1}\right) \{T^2\}$$

or,

$$\{T\} = N_{\tau_1}\{T^1\} + N_{\tau_2}\{T^2\} \qquad \dots (5.30)$$

N_{τ_1}, N_{τ_2}, as given in eq. (5.30), are the shape functions in the time domain.

5.4.2 Matrix Relation

We substitute expression (5.30) for vector $\{T\}$ in eq. (5.27). Since only two time instants are involved we can take the initial time instant as zero and the final one as $\Delta\tau$. Then

$$\int_0^{\Delta\tau} N_{\tau_2}\left[[H'](N_{\tau_1}\{T^1\}+N_{\tau_2}\{T^2\})\right.$$
$$\left.+[C]\left(\{T^1\}\frac{\partial N_{\tau_1}}{\partial\tau}+\{T^2\}\frac{\partial N_{\tau_2}}{\partial\tau}\right)+\{f\}\right]d\tau=0 \quad \ldots (5.31)$$

where

$$N_{\tau_1}=\frac{\Delta\tau-\tau}{\Delta\tau};\ N_{\tau_2}=\frac{\tau}{\Delta\tau}$$

On integration this gives,

$$[H']\left\{\frac{\Delta\tau}{6}\{T^1\}+\frac{\Delta\tau}{3}\{T^2\}\right\}+[C]\left\{-\frac{1}{2}\{T^1\}+\frac{1}{2}\{T^2\}\right\}+\frac{\Delta\tau}{2}\{f\}=0$$

or

$$\{T^2\}=-\left[\frac{2}{3}[H']+\frac{1}{\Delta\tau}[C]\right]^{-1}\left\{\left[\frac{1}{3}[H']-\frac{1}{\Delta\tau}[C]\right]\{T^1\}+\{f\}\right\} \ldots (5.32)$$

The matrix relation (5.32) gives the temperature vector $\{T^2\}$ at the end of time step $\Delta\tau$ in terms of known temperatures given as vector $\{T^1\}$ at the start of the time step. Knowing $\{T^2\}$ we can determine $\{T^3\}$ at the end of the next time step using $\{T^2\}$ as the temperatures at the start of the step and thus proceed for subsequent steps.

In this section we have used the Galerkin method to write the weighting function in terms of shape function. Other procedures could also be used but the Galerkin method has been found to give the best results.

5.5 ILLUSTRATIVE EXAMPLES

5.5.1 Resistance Spot Welding

Unsteady-state heat-flow analysis, formulated for the axi-symmetric case, has been used [1] to determine temperature distribution in the electrode-sheet system of resistance spot welding. Figure 5.6 shows discretization of the domain comprising a copper electrode and steel sheets. Fine mesh is used in the sheet as well as contact surface because rapid temperature gradients exist there. Flow of heavy current for a short duration results in rapid heating of the interface due to high contact resistance. Although sheet metal (mild steel) has low resistivity, the flow of very heavy current results in bulk heating of the sheet especially because resistivity increases with rise in temperature. Electrical field analysis is required to determine Joule heat in the bulk of the sheet and resistive heating at the interface of

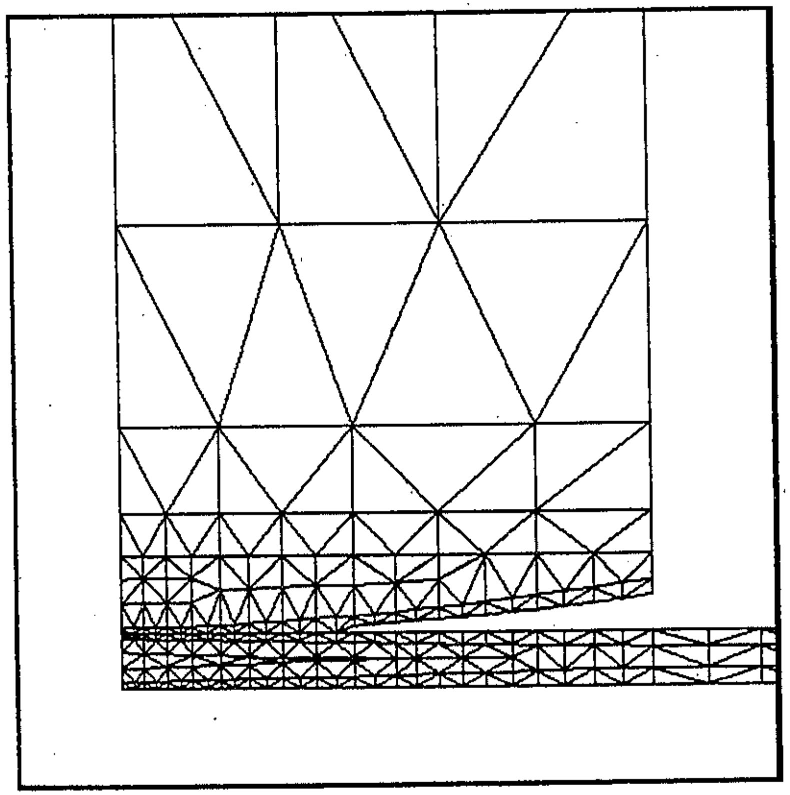

Fig. 5.6 Discretization of electrode and sheet in resistance welding.

it. Moreover, contact resistance varies due to flattening of microlevel irregularities on the surface of the sheet as well as due to heating. It was modelled while considering appropriately the state of stress at the interface. Final temperature rise, melting and growth of fusion zone (nugget) as well as the cooling rates were determined. A few such plots at different instants of time during resistance spot welding are shown in Fig. 5.7.

5.5.2 Heat Transfer in Piston-Cylinder Assembly of Automobile Engine

Studies on the combustion cycle in diesel engines have revealed an improvement in efficiency when the overall combustion chamber temperature is high. This has resulted in development of low-heat-rejection (LHR) diesel engines in which a plasma-sprayed ceramic lining is applied on the inside of the cylinder and top of the piston[2]. Ceramic coating

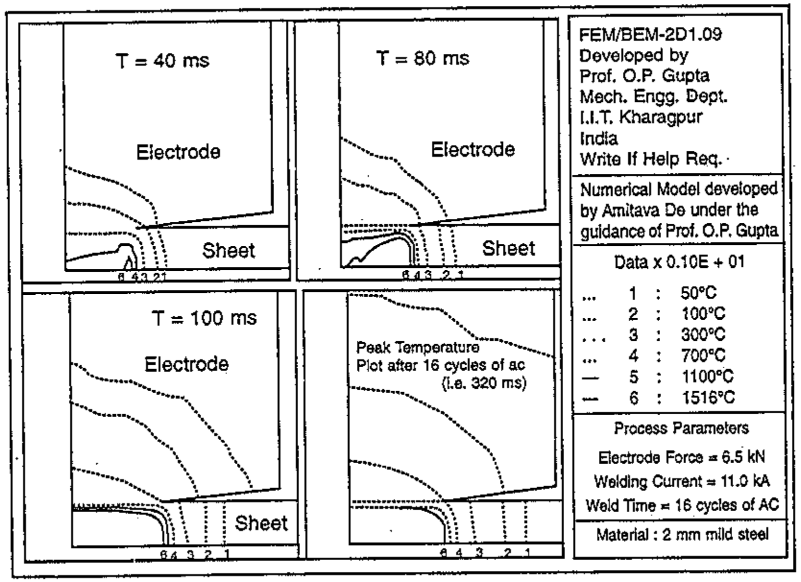

Fig. 5.7 Isothermal contour plot at different instants of time and peak temperature plot in resistance welding

results in low heat rejection to the cylinder while maintaining high temperature inside the combustion chamber. This reduces engine cooling requirement but at the same time steep temperature gradients are produced in the ceramic coating, which leads to its cracking. The study of heat flow in this system provides vital information on temperature distribution and its gradients, which help in subsequent analysis of the lubricating behaviour of engine oil at that temperature and other associated features of engine performance. Such a study was reported by Assanis and Badillo [2]. This study also provides useful guidelines for modelling heat transfer phenomena in real systems.

(a) Salient features of FE model: A schematic diagram of one cylinder of the engine is shown in Fig. 5.8(a). The configuration and boundary conditions being symmetrical about the axis, an axi-symmetric analysis was done. The nature of the mesh used in this system is shown in Fig. 5.8(b) where a very fine mesh is used in 2-mm thick ceramic coating. The mesh size was 0.1 mm for elements exposed to the combustion chamber and was gradually increased inwards as shown for the piston in this Figure. A total of 382 elements and 254 nodes were used. Since the gas temperature in the combustion chamber varied during the cycle, it was determined through a separate simulation model for different positions

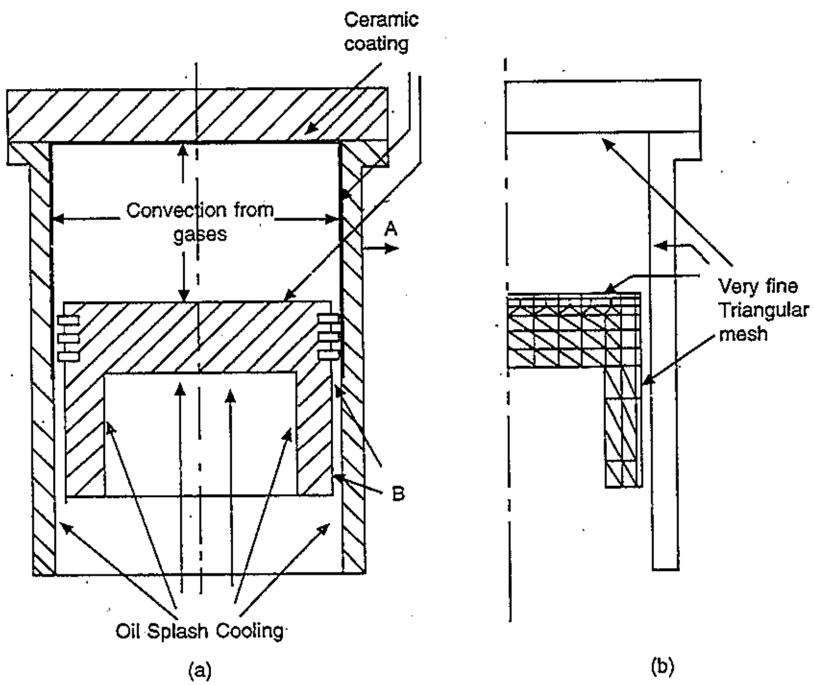

A—Convection to cooling water
B—Conduction through oil and gas film

Fig. 5.8 Heat transfer analysis of diesel engine: (a) General configuration; (b) F.E. Mesh

of the piston. The crucial aspect of heat transfer through various surfaces was resolved as follows.

(i) Heat transfer from hot gases to the cylinder head, piston top and a portion of the cylinder liner was modelled using a temperature dependent convective heat-transfer coefficient which was modified to include the effect of radiation.

(ii) An average value of 2 μm was taken as the thickness of lubricating oil film between cylinder liner and piston ring based on past data. The radial clearance between piston and cylinder was 100 μm and heat transfer through this region was assumed to occur by convection through the oil film. The thermal conductivity of this lubricating medium was taken as 0.12 W/m.K.

(iii) The bottom side of the piston and cylinder liner was assumed to be exposed to splash cooling through oil in the crankcase. The temperature of this oil and surface heat-transfer coefficient was taken as 380 K and 1500 W/m^2.K respectively.

(iv) The cylinder liner was cooled through water circulating around it with the surface heat-transfer coefficient taken as 5000 $W/m^2.K$ and water temperature as 380 K.

(v) Finite element analysis was performed in two stages. During the initial first stage a steady-state analysis was performed using an average heat-transfer coefficient and mean gas temperature. This was necessary in order to establish the initial conditions for start of the iteration process for subsequent unsteady-state heat-transfer analysis. Later, the analysis was performed for different piston positions during the engine cycle while using the instantaneous values of combustion gas temperature and its enhanced heat-transfer coefficient for each such piston positions. The program was iterated through a series of complete engine cycles until the nodal temperatures for each piston position came within a permissible range with respect to the same piston position as in the previous cycle.

(vi) The temperatures so calculated at the surface of the ceramic coating on the piston varied within 700–900 K compared to similar variation for an uncoated piston within the range of 540–580 K.

The basic features of the analysis are the extreme care taken during modelling of surface heat-transfer conditions (boundary conditions) along different regions and the fine grid used at critical locations. Needless to say, the accuracy of such calculations depends greatly on the way boundary conditions and other real effects are simulated.

REFERENCES

1. Gupta, O.P. and De, A. (1998). An Improved Numerical Modelling for Resistance spot welding process and its experimental verification. Trans. ASME, J. of Mfg. Sc. and Engg., v 120, pp. 246–251.
2. Assanis, D.N. and Badillo, E. (1988). 'Transient analysis of piston-liner heat transfer in low-heat-rejection Diesel engines'. SAE Transactions, *J. for Engines*. Paper No. 880189, pp. 6.295–6.305.

Chapter 6

BEAMS, PLATES AND SHELLS

6.1 INTRODUCTION

Beams and plates form important elements of structures, pressure vessels and machines. Analysis of indeterminate structures formed of beams of uniform and non-uniform cross-section subjected to various types of loading including bending, twisting or direct load calls for very special efforts and the finite element method comes in very handy in these situations. Automobile chassis, cranes, underframe of railway bogies and machine beds are a few typical examples from the field of mechanical engineering besides building structures, bridges etc. which can be analyzed using beam elements. All pressure vessels containing gas or liquid under pressure, boilers, submarines, ship decks and machine frames are examples of plate structures. The complex configuration and nature of loading makes the finite element technique the only viable approach for solving such problems. Problems of sheet metal forming of automobile body parts (including its die design) have also been tackled using large-displacement plate bending analysis [1, 2]. Beam and plate problems are similar in that both are loaded in bending and other types of stress may often play a secondary role. This makes the form of deflection expression and subsequent analysis similar in the two cases.

6.2 BENDING OF BEAMS

A beam of non-uniform cross-section loaded in the transverse direction is shown in Fig. 6.1. It is divided into elements, such as 1-2, 2-3 etc. One of the elements (say 2-3) is redrawn in Fig. 6.2 and is denoted as 1-2 for convenience. We shall analyze the stresses due to bending of this element. Before that let us define a few related quantities, such as bending moment, slope, deflection, rotation and the sign conventions for these. Generally the beam, subjected to bending, is assumed to deflect in a plane passing through the neutral axis. If the beam is aligned along the x-axis, it may deflect either in x-z or x-y planes, as shown in Fig. 6.2(i) and (ii) respectively. These Figures also show the three coordinate axes.

Considering Fig. 6.2(i), deflection of the beam in z-direction is designa-